

Mitochondrial Dysfunction Causing Cardiac Sodium Channel Downregulation in Cardiomyopathy

Man Liu^{1,2}, PhD; Lianzhi Gu^{1,2}, MD, PhD; Matthew S. Sulkin³, MS; Hong Liu^{1,2}, MD, PhD; Euy-Myoung Jeong¹, PhD; Ian Greener¹, PhD; An Xie¹, PhD; Igor R. Efimov³, PhD; Samuel C. Dudley^{1,2}, Jr. MD, PhD
¹Section of Cardiology, Department of Medicine, University of Illinois at Chicago; ²the Jesse Brown VAMC, Chicago, IL, USA; and ³Department of Biomedical Engineering, Washington University in Saint Louis, USA

Address correspondence to:

Dr. Samuel C. Dudley
Section of Cardiology
University of Illinois at Chicago/Jesse Brown VA Medical Center
840 S. Wood Street, MC715
Chicago, IL 60612
Phone: 1-312-413-8870
FAX: 1-312-413-2948
Email: scdudley@uic.edu

Abstract

Cardiomyopathy is associated with cardiac Na⁺ channel downregulation that may contribute to arrhythmias. Previously, we have shown that elevated intracellular NADH causes a decrease in cardiac Na⁺ current (I_{Na}) signaled by an increase in mitochondrial reactive oxygen species (ROS). In this study, we tested whether the NADH-mitochondria ROS pathway was involved in the reduction of I_{Na} in a nonischemic cardiomyopathic model and correlated the findings with myopathic human hearts.

Nonischemic cardiomyopathy was induced in C57BL/6 mice by hypertension after unilateral nephrectomy, deoxycorticosterone acetate (DOCA) pellet implantation, and salt-water substitution. Sham operated mice were used as controls. After six weeks, heart tissue and ventricular myocytes isolated from mice were utilized for whole-cell patch clamp recording, NADH/NAD⁺ level measurements, and mitochondrial ROS monitoring with confocal microscopy. Human explanted hearts were studied using optical mapping.

Compared to the sham mice, the arterial blood pressure was higher, the left ventricular volume was significantly enlarged (104.7 ± 3.9 vs. 87.9 ± 6.1 μ L, $P < 0.05$), and the ejection fraction was reduced ($37.1 \pm 1.8\%$ vs. $49.4 \pm 3.7\%$, $P < 0.05$) in DOCA mice. Both the whole cell and cytosolic NADH level were increased ($279 \pm 70\%$ and $123 \pm 2\%$ of sham, respectively, $P < 0.01$), I_{Na} was decreased ($60 \pm 10\%$ of sham, $P < 0.01$), and mitochondrial ROS overproduction was observed (2.9 ± 0.3 -fold of sham, $P < 0.01$) in heart tissue and myocytes of myopathic mice vs. sham. Treatment of myocytes with NAD⁺ (500 μ M), mitoTEMPO (10 μ M), chelerythrine (50 μ M), or forskolin (5 μ M) restored I_{Na} back to the level of sham. Injection of NAD⁺ (100 mg/kg) or mitoTEMPO (0.7 mg/kg) twice (at 24 h and 1 h before myocyte isolation) to animals also restored I_{Na}. All treatments simultaneously reduced mitochondrial ROS levels to that of controls. CD38 was found to transduce the extracellular NAD⁺ signal. Correlating with the mouse model, failing human hearts showed a reduction in conduction velocity that improved with NAD⁺.

Nonischemic cardiomyopathy was associated with elevated NADH level, PKC activation, mitochondrial ROS overproduction, and a concomitant decrease in I_{Na}. Reducing mitochondrial ROS by application of NAD⁺, mitoTEMPO, PKC inhibitors, or PKA activators, restored I_{Na}. NAD⁺ improved conduction velocity in human myopathic hearts.

Abbreviations and Acronyms:

AIP, autocalmitide-2 related inhibitory peptide
 β -AR, β -adrenergic receptor
CaMKII, calcium/calmodulin-dependent protein kinase II
CV, conduction velocity
DOCA, deoxycorticosterone acetate
GPD1L, glycerol-3-phosphate dehydrogenase 1 like
I_{Na}, cardiac Na⁺ current
LV, left ventricle
NAD⁺, β -nicotinamide adenine dinucleotide
NADH, reduced form of nicotinamide adenine dinucleotide
Na_v1.5, cardiac sodium channel
PK, protein kinase
ROS, reactive oxygen species
SCN5A, cardiac sodium channel gene

1. Introduction

Despite extensive research and novel treatments, conditions associated with deranged cardiac metabolism, such as heart failure or ischemia, are accompanied still by a substantial risk of arrhythmic sudden death [1]. While implanted cardiac defibrillators have decreased sudden death risk, they can cause physical and psychological complications. They are also expensive, and do not address the underlying pathology that leads to arrhythmic risk [2, 3]. A more complete molecular understanding of the basis for the increased arrhythmic risk is likely to lead to new therapies that will be more effective and less invasive.

Cardiac injury from many causes is associated with altered metabolism and downregulation of the cardiac Na^+ channel ($\text{Na}_v1.5$) [4-7]. Recently, we reported that an elevation of intracellular reduced nicotinamide adenine dinucleotide (NADH) can downregulate Na^+ current (I_{Na}) acutely and to a degree that is large enough to be clinically significant [8]. The signaling cascade involves a protein kinase C (PKC)-mediated increase in mitochondrial reactive oxygen species (ROS) production [9, 10]. NADH is known to oscillate with myocardial ischemia, and mitochondrial injury is associated with increased NADH and ROS levels [11, 12]. These changes could contribute to reduced I_{Na} , conduction block, and arrhythmic risk known to exist with reduced cardiac contractility. The NADH effect on ROS production and I_{Na} can be antagonized by PKA activation mediated by NAD^+ , by superoxide dismutase, or by mitoTEMPO, a specific scavenger of mitochondrial ROS [9, 10]. To evaluate the clinical relevance of this signaling pathway, we tested whether NADH and mitochondrial ROS were elevated in nonischemic cardiomyopathy and whether these changes resulted in a reduction in I_{Na} . We also investigated whether NAD^+ , mitoTEMPO, PKC inhibitors (a PKC pan inhibitor chelerythrine and $\delta\text{V1-1}$, a specific inhibitor for PKC δ), or a PKA activator (forskolin) could counteract the effects of NADH on mitochondrial ROS and cardiac I_{Na} . We evaluated the role of the β -adrenergic receptor (β -AR), CD38, and the purinergic receptor [13-16], to determine how extracellular NAD^+ , which is membrane impermeable, affected I_{Na} . To show relevance of the findings, the effect of NAD^+ on conduction velocity (CV) in human failing hearts was evaluated.

2. Materials and Methods

2.1. Model generation and isolation of mice ventricular myocytes

Nonischemic cardiomyopathy was induced in C57BL/6 mice by six weeks of hypertension evoked after unilateral nephrectomy, deoxycorticosterone acetate (DOCA) pellet implantation (0.7 mg/day, Innovative Research of America, Sarasota, FL), and 1% salt water substitution [17]. Sham operated mice were used as controls. Ketamine (100 mg/kg) and xylazine (10 mg/kg) were administered by intraperitoneal pre-operation and buprenorphine (0.1 mg/kg) was injected subcutaneously post-operation and at 12-hour interval as needed. For each experiment, three to eight mice were used.

Ventricular myocytes were isolated as described before [17, 18]. Briefly, hearts were excised from anesthetized mice, perfused with perfusion buffer (in mM: NaCl 113, KCl 4.7, Na₂HPO₄ 0.6, KH₂PO₄ 0.6, MgSO₄ 1.2, Phenol Red 0.032, NaHCO₃ 12, KHCO₃ 10, HEPES 10, Taurine 30, 2-3-butanedione monoxime 10) and digested with collagenase II (Worthington Biochemical Co. Lakewood, NJ). Cardiomyocytes were washed with control buffers (in mM: NaCl 133.5, KCl 4, Na₂HPO₄ 1.2, HEPES 10, MgSO₄ 1.2) with serially increasing Ca²⁺ concentrations (0.2, 0.5, and 1 mM). Then, myocytes were incubated in MEM medium (modified Eagle's medium with 1% insulin-transferrin-selenium, 0.1% bovine serum albumin, 1% L-glutamine, and 1% penicillin/streptomycin) in a 95% O₂/5% CO₂ incubator at 37 °C for 2 hours prior to being used for patch clamp recording and ROS level measurements.

2.2. Documentation of cardiomyopathy

Blood pressure and heart rate were measured on acclimated conscious mice six weeks after surgery using tail-cuff plethysmography (Columbus Instruments, Columbus, Ohio). Transthoracic echocardiography was performed using the Vevo 770 system equipped with a RMV-707B transducer (VisualSonics, Toronto, Canada). Mice were anesthetized with 1% isoflurane in oxygen and were closely monitored during the procedure. Images were obtained from the parasternal long axis view and parasternal short axis view at the midpapillary level. Wall thickness, chamber size, fractional shortening (%FS), and ejection fraction (%EF) were evaluated by two-dimensional and M-mode echocardiography. Measurements were averaged from three consecutive beats.

2.3. Whole cell and cytosolic NADH and NAD⁺ levels

We measured both whole cell and cytosolic NADH and NAD⁺ levels of mouse heart tissue from sham and DOCA mice. We also tested whether injection of NAD⁺ to sham and DOCA mice (100 mg/kg, twice at 24 h and 1 h before heart harvest) affected the cytosolic NADH and NAD⁺ levels. Four animals were used for each group. The cytosol of cardiomyocytes was isolated from mitochondria with the Mitochondria Isolation Kit for Tissue (Pierce Biotechnology, Rockford, IL) by following the manufacturer's protocol. The EnzyChromTM NAD⁺/NADH Assay Kit (BioAssay Systems, Hayward, CA) was used to measure NADH and NAD⁺ levels from whole cells and cytosol according to the manufacturer's instructions. The absorption intensity difference of the reduced product color, measured at 565 nm at time zero and 15 min later, was used to calculate NADH and NAD⁺ levels.

2.4. Cellular electrophysiology

Na⁺ currents of ventricular myocytes were measured using the whole-cell patch clamp technique in voltage-clamp mode at room temperature [9, 10]. To measure Na⁺ currents, pipettes (1-2 MΩ) were filled with a pipette solution containing (in mM): CsCl 80, cesium aspartate 80, EGTA 11, MgCl₂ 1, CaCl₂ 1, HEPES 10, and Na₂ATP 5 (adjusted to pH 7.4 with CsOH). The bath solution consisted of (in mM): NaCl 15, CsCl 5, CaCl₂ 1, MgCl₂ 1, tetramethylammonium Cl 20, N-methyl-D-glucamine 100, 4-aminopyridine 3, MnCl₂ 2, HEPES 10 and glucose 10 (adjusted to pH 7.4 with CsOH). To measure current, a stepped voltage protocol from -100 to +60 mV with a holding potential of -100 mV was applied to establish the presence of Na_v1.5. Peak currents obtained during steps to -20 mV were used for comparison in determining the relative reduction of I_{Na}. To minimize time-dependent drift in gating parameters, all protocols were initiated 2-5 min after whole-cell configuration was obtained. The currents were normalized with cell capacitance.

To measure the resting membrane potential, perforated current-clamp was performed on isolated myocytes from sham and DOCA mice [19]. The pipette solution contained (in mM): potassium gluconate 120, KCl 20, NaCl 5, HEPES 5, MgATP 5, and β -escin 0.03 (adjusted to pH 7.2 with KOH). The bath solution consisted of (in mM): NaCl 140, KCl 5.4, MgCl₂ 1, HEPES 5, CaCl₂ 1.8, and glucose 5.5 (adjusted to pH 7.4 with NaOH). Pipette resistance were 3-5 M Ω .

2.5. Measurement of mitochondrial ROS

To measure mitochondrial ROS, the fluorescent probe MitoSOXTM Red (Invitrogen) was used according to the manufacturer's protocol. Briefly, ten groups of isolated cardiomyocytes were studied: sham mouse myocytes, DOCA mouse myocytes, and myocytes from sham or DOCA mice treated with 500 μ M NAD⁺, 10 μ M mitoTEMPO, 2 μ M δ V1-1, or 5 μ M forskolin for 10-min at 37 °C. Cells were then washed once with MEM and incubated with 5 μ M MitoSOXTM Red and 100 nM MitoTracker Green (Invitrogen) for 10 min at 37 °C, followed by washing three times with MEM medium. Images were taken on a Zeiss LSM710 confocal microscope (Carl Zeiss GmbH, Germany) using an argon laser excitation (514 nm) with emission collection through a 560 nm long pass filter. The mean values of the whole cell fluorescence of MitoSOXTM Red were obtained with ImageJ software.

For flow cytometry measurements, isolated cardiomyocytes from sham or DOCA mice injected with 100 mg/kg NAD⁺ or with 0.7 mg/kg mitoTEMPO twice (at 24 h and 1 h before myocyte isolation, respectively) were incubated with MitoSOXTM Red (5 μ M) for 15 min and washed twice with MEM. Appropriate gating was used to select cardiomyocytes, and ~10,000 cells were read in each sample at FL-2 in CyAN ADP flow cytometry (Beckman-Coulter, Brea, CA).

2.6. Biotinylation and Western blotting of Na_v1.5

Analysis of Na⁺ channels present at the cell surface was performed on freshly isolated cardiomyocytes of sham and DOCA mice as previously described with the Pierce[®] Cell Surface Protein Isolation Kit (Pierce Biotechnology, Rockford, IL) [20]. For detection of Na_v1.5, the primary antibody (rabbit anti-SCN5A, Alomone Labs, Jerusalem, Israel) was diluted 1:200. Horseradish peroxidase-conjugated goat anti-rabbit IgG secondary antibody (Cell Signaling Technology, Danvers, MA) was diluted 1:5000. Actin (Santa Cruz Biotechnology, CA) was used as a loading control. Six animals were used for each group.

2.7. SCN5A RNA abundance

Total RNA was isolated (RNeasy Minikit – Qiagen, Valencia, CA) from snap frozen ventricular tissue samples taken from sham and DOCA mice (n=3 per group). Equal quantities of total RNA from all samples were used to generate cDNA using the High Capacity cDNA synthesis kit (Applied Biosystems, Carlsbad, CA), and quantitative PCR was performed using Fast SYBR green chemistry (Applied Biosystems, Carlsbad, CA) on an ABI 7500 platform. Primers were designed against mouse SCN5A (SCN5A_F TTGCTCCTTCTCATGGTTG and SCN5A_R CATGGAGATGCTCAAGAAGGA) and Hypoxanthine phosphoribosyltransferase (HPRT) (HPRT_F AGGCCAGACTTTGTTGGATTT and HPRT_R GGCTTTGTATTGGCTTTTCC) using Primer3 plus software (<http://www.bioinformatics.nl/cgi-bin/primer3plus>) and synthesized by MWG (Huntsville, AL). HPRT acted as the housekeeping gene by which to normalize SCN5A cDNA. The 2^{- $\Delta\Delta$ Ct} method was used for relative quantification between groups. A t-test was used for test for statistical comparison between the two groups.

2.8. Conduction velocity measurement with human failing heart tissue

Failing human hearts (n=3) of different cardiomyopathies (supplemental data) were provided by Barnes-Jewish Hospital (Washington University in Saint Louis, Mo) and non-failing donor hearts (n=2) were provided by Mid-America Transplant Services (Saint Louis, MO) for comparative purposes. Optical mapping experiments of human hearts were done as previously described [21, 22]. Briefly, left ventricular (LV) wedge preparations were isolated from the posterior-lateral LV free wall and perfused through the left marginal artery with Tyrode's solution. Tissue was stained with di-4-ANNEPS (15 μ M;

Molecular Probes, Eugene, Oregon) for recording optical action potentials and was immobilized by addition of blebbistatin (10-20 μM ; Tocris Bioscience, Ellisville, MO) to reduce motion artifact.

LV wedge preparations were paced at the sub-endocardium at twice the diastolic pacing threshold with a 5-ms pulse width. A restitution pacing protocol was conducted, in which pacing started at 2000 ms and decreased until the ventricular functional refractory period was reached. Following control pacing, NAD^+ (500 μM) was bolus-injected into a drug port. Tissue was allowed to stabilize for 25-30 minutes and then a second restitution pacing protocol was performed. Data was analyzed using custom MATLAB software [23]. All optical data were filtered using a 3×3 pixel spatial filter and a 0-100 Hz finite impulse response filter. Activation times were defined as the maximum first derivative of the fluorescent signal and CV was calculated as described by Bayly et al. [24]. The magnitude of CV was determined to be the median conduction calculated in the region of interest (Fig. 6D middle). The Student's paired t-test was used to determine the level of statistical significance ($P<0.05$).

2.9. Statistical evaluations

Data are shown as the mean \pm SEM. Aside from above, determinations of statistical significance were performed with ANOVA with the Bonferroni correction for comparisons of multiple means. A value of $P<0.05$ was considered statistically significant.

3. Results

At six weeks after surgery, DOCA mice had developed hypertension and systolic heart dysfunction confirmed by tail-cuff blood pressure measurements and echocardiography. As shown in Table 1, compared to the sham mice, DOCA mice showed higher artery blood pressure, enlarged left ventricular chamber (105 ± 4 vs. 88 ± 6 μ L of sham, $P < 0.05$), and reduced ejection fraction ($37 \pm 2\%$ vs. $49 \pm 4\%$ of sham, $P < 0.05$).

3.1. Elevated NADH level in cardiomyopathic heart tissue

We measured whole cell and cytosolic NADH and NAD^+ levels of sham and DOCA mice hearts, before and after treatment with NAD^+ . Fig. 1 shows the ratios of whole cell and cytosolic NADH and NAD^+ levels, and NADH/NAD^+ . The whole cell and cytosolic NAD^+ levels of the sham and DOCA groups were similar. On the other hand, NADH was increased $279 \pm 70\%$ for whole cell and $123 \pm 2\%$ for cytosol in DOCA mice ($P < 0.01$ vs. sham for both). Consistent with the hypothesis that cytosolic NADH changes mediate the effects on I_{Na} , DOCA mice injected with NAD^+ showed a similar cytosolic NADH level as the sham group ($110 \pm 8\%$ of sham, $P > 0.05$). Injection of NAD^+ had no influence on cytosolic NADH and NAD^+ levels in sham mice. The cytosolic NADH/NAD^+ ratios of all groups were similar, although the whole cell NADH/NAD^+ ratio of DOCA group was increased $220 \pm 69\%$, compared to the sham group. According to our previous work, an increase in intracellular NADH level could lead to significant decrease of I_{Na} [9]. Therefore, we measured the I_{Na} of isolated myocytes of sham and DOCA mice.

3.2. Decreased I_{Na} in cardiomyopathic ventricular cardiomyocytes

Fig. 2A shows representative traces of I_{Na} measured from isolated sham and DOCA ventricular myocytes. The I_{Na} of DOCA myocytes was decreased significantly. Fig. 2B presents the averaged peak currents measured at -20 mV with a holding potential of -100 mV, I_{Na} of the cardiomyopathy group being $60 \pm 10\%$ of the sham ($P < 0.01$). While we did not measure serum Na^+ changes induced by DOCA treatment, the anticipated increase is not likely to compensate for the reduced current observed in the patch clamp experiments nor is it likely that the reduction in current observed is in compensation for this anticipated small increase in driving force for Na^+ entry.

The decrease in I_{Na} was not related to changes in transcription, because quantification of SCN5A mRNA revealed no significant difference in transcript levels with the sham and DOCA heart tissue ($P = 0.95$). To investigate $\text{Na}_v1.5$ membrane expression, we labeled channels present on the membrane surface with biotinylation. Western blot analysis for biotinylated Na^+ channels showed no significant difference between sham and DOCA mice as in Fig 3: 1.63 ± 0.21 vs. 1.39 ± 0.19 , $n = 6$ for each group, $P = 0.42$. The resting membrane potential of DOCA mice myocytes (-78.3 ± 5.0 mV) was not altered compared to the sham group (-75.5 ± 0.8 mV, $P > 0.05$).

3.3. Restoring I_{Na}

In our previous studies on ventricular cells from normal hearts, NAD^+ , mitoTEMPO, chelerythrine and forskolin reversed a NADH-induced decrease of I_{Na} [9, 10]. In this work, intracellular application of NAD^+ , mitoTEMPO, chelerythrine, or forskolin (500, 10, 50, or 5 μ M, respectively) to isolated myocytes of cardiomyopathic mice restored I_{Na} from $60 \pm 10\%$ to $97 \pm 7\%$, $93 \pm 8\%$, $112 \pm 86\%$, $109 \pm 6\%$ of sham at -20 mV, respectively (Fig 4A and 4C, $P > 0.05$). As shown in Fig. 4A and 4B, there were minor shifts of $V_{1/2}$ values of steady state activation and inactivation, but they were not enough to affect the evaluation of the peak currents. Treatment of sham myocytes with these compounds had no influence on I_{Na} (data not shown).

Treating animals with NAD^+ and mitoTEMPO had similar effects as applying these compounds to isolated myocytes. We injected the animals twice with NAD^+ (100 mg/kg) or mitoTEMPO (0.7 mg/kg), at 24 hours and 1 hour before the myocyte isolation. As shown in Fig 4D and 4F, NAD^+ or mitoTEMPO completely restored the decreased I_{Na} seen in myopathic myocytes ($115 \pm 9\%$ and $119 \pm 9\%$ of sham injected with NAD^+ or mitoTEMPO, respectively, at -20 mV, $P > 0.05$). As shown in Fig. 4D and 4E, there were also minor shifts of $V_{1/2}$ values of steady state activation and inactivation that were not enough

to affect the evaluation of the peak currents. There were subtle differences in the response of Na⁺ channel kinetics to treatment in vivo and in vitro. The origin and the significance of these differences are unknown. Doses for the treatment drugs were based on demonstration of maximal I_{Na} recovery in vitro. The lack of difference between in vitro and in vivo treatment effects suggests the doses used in vivo were also sufficient to induce a maximal effect.

3.4. Mitochondrial ROS are increased in myopathic ventricular myocytes

Previously, we have shown that elevated NADH increases mitochondrial ROS production, causing a reduction of Na⁺ current [9, 10]. To test if this mechanism of the I_{Na} reduction was similar in a clinically relevant model, MitoSOXTM Red was used to demonstrate mitochondrial ROS production in myopathic ventricular myocytes of DOCA mice. As shown in Fig. 5A, the mitochondrial ROS level of myopathic myocytes increased 2.9 ± 0.3-fold (P<0.01 vs. sham). This is similar to a four-fold increase of superoxide production observed in the aortas of DOCA mice [25].

Treatment of myocytes with NAD⁺, mitoTEMPO, δV1-1, or forskolin (500, 10, 2, or 5 μM, respectively) extracellularly led to decreases of ROS in myopathic mouse myocytes to levels similar to the sham group (1.4 ± 0.1, 1.1 ± 0.1, 0.9 ± 0.1, or 0.8 ± 0.1-fold of sham, respectively, P>0.05). Here, we used the specific inhibitor of PKCδ, δV1-1, instead of chelerythrine, because chelerythrine's fluorescence affected the evaluation with MitoSOXTM Red. Fig. 5C shows representative confocal images of these measurements. Treatment of sham myocytes with these compounds had no effect on mitochondrial ROS production (data not shown). For the animal treated groups, we used flow cytometry to test the MitoSOXTM Red fluorescence. This method measured ~ 10,000 myocytes for each group to produce more reliable measure of net mitochondrial ROS. Similar results to those with confocal microscopy were obtained with sham, DOCA and DOCA mice injected with NAD⁺ or mitoTEMPO (100 or 0.7 mg/kg, respectively; Fig 5B). The mean fluorescent intensity of the myopathic DOCA group was increased by 1.7 ± 0.1-fold when compared to sham (P<0.05). NAD⁺ and mitoTEMPO decreased the mitochondrial ROS overproduction in myopathic mouse myocytes to 1.1 ± 0.2- and 1.0 ± 0.1-fold of sham, respectively (P>0.05).

3.5 Extracellular NAD⁺ signals mainly through CD38

We evaluated the role of the β-adrenergic receptor (β-AR), CD38, and the purinergic receptor [13-16], to determine how extracellular NAD⁺, which is membrane impermeable, affected I_{Na}. NADH applied in the pipette solution induced a 62±4% reduction of I_{Na} at -20 mV. NAD⁺ recovered the decreased I_{Na} to 93±3% of control. Specific inhibitors for CD38 (pelargonidin at 160 μM) [26], β-AR (Nadolol at 20 μM) [27, 28], and purinergic receptors (suramin at 100 μM) [29, 30] were applied respectively to the extracellular solution for 15 min (pelargonidin or Nadolol) or 1 hour (suramin) before addition of NAD⁺. With pelargonidin, nadolol, and suramin, the I_{Na} upon application of NAD⁺ returned to 63±5% (P<0.01 vs. control), 80±5% (P<0.05 vs control) and 102±7% (P>0.05 vs. control) of control, respectively. The inhibitors did not affect the cardiac I_{Na} when applied separately (data not shown). Therefore, we conclude that mainly CD38 mediates the NAD⁺ effect to recover I_{Na}. The β-AR might play a minor role in the NAD⁺ effect, while the purinergic receptors do not appear to contribute to this signaling pathway.

3.6 NAD⁺ improved the conduction velocity of human failing hearts

We tested the clinical relevance of the DOCA mouse model findings in isolated human heart tissue. CV from non-failing and failing hearts were similar to what has been previously reported [31]. Failing hearts showed a reduction in CV that improved with NAD⁺. For both failing (n=3) and non-failing (n=2) human hearts, CV was calculated both before and after administration of NAD⁺ at several pacing cycle lengths (2000, 1000, 800, 600 ms). Fig. 6A shows a representative LV wedge preparation with key features highlighted. The dotted white line indicates the field of view of activation and CV maps (Fig. 6C and 6D left), where the CV was calculated within the teal rectangle. Blue and green circles in Figure 6A specify the location of representative optical action potentials seen in Fig. 6B. The activation map in Fig. 6C depicts the spread of electrical propagation from the location of the pacing electrode near the sub-endocardium (blue) to the epicardial surface (red).

In Fig. 6D CV vectors (red arrows) are displayed on top of an activation map in gray scale. The center panel magnifies the area (teal box) where the magnitude of CV was determined at all cycle lengths (2000, 1000, 800, 600 ms) for individual wedge preparations. The mean values of CV of failing hearts and control hearts before and after administration of NAD⁺ are listed in Table 2. After addition of NAD⁺, the CV of failing heart increased at all cycle lengths and was significantly different at three cycle lengths (2000 ms: P=0.02, 800 ms: P=0.0006, and 600 ms: P=0.003).

4. Discussion

Voltage-gated Na⁺ channels are responsible for generating the main current for excitation propagation in the membrane of most excitable cells, such as cardiomyocytes and neurons [32, 33]. Cardiac Na⁺ channel changes have been implicated in the increased risk of sudden death in heart failure [34-36]. In our previous studies on the mechanism by which mutations in glycerol-3-phosphate dehydrogenase 1 like (GPD1L) protein cause reduced I_{Na} and Brugada Syndrome, we have shown that increased cytosolic NADH can downregulate the cardiac Na⁺ channel through PKC activation and mitochondrial ROS overproduction [9, 10]. Here, we demonstrated that the metabolic derangements occurring in cardiomyopathy resulted in reductions in I_{Na} by a similar mechanism. Hypertensive DOCA mice presented enlarged left ventricular chamber and reduced ejection fraction associated with elevated cytosolic NADH level, increased mitochondrial ROS, and reduced I_{Na}. The reduction in I_{Na} was on the order of magnitude seen in Brugada Syndrome. These results reveal links between mitochondrial dysfunction with ROS overproduction, downregulation of cardiac Na_v1.5, and nonischemic cardiomyopathy. The heart tissue of DOCA mice showed no change in SCN5A mRNA abundance or Na_v1.5 protein membrane expression. The reason for decreased I_{Na} is, therefore, not a decrease of Na_v1.5 channel number, but decreases of the probability of channel opening or of the single channel conductance. Sirtuins are pyridine nucleotide-dependent histone deacetylases or mono-ribosyltransferases. Given the time scale of the changes in I_{Na} in response to NADH, it is unlikely that a sirtuin-dependent transcriptional change is responsible for the effects observed. Nevertheless, a direct effect of sirtuins on the channel cannot be excluded. The increase in cardiac mitochondrial ROS is consistent with other studies showing that DOCA-salt treatment increases ROS production in the aorta of DOCA hypertension mice [17, 25] and rats [37, 38].

The improved CV of human failing heart by administration of NAD⁺ was consistent with the changes in I_{Na} seen in the DOCA mouse model based on the cable equation, where the CV is proportional to I_{Na}^{1/8}. The ratio of CV of the failing hearts versus NAD⁺-treated failing hearts is 1.05 – 1.08 at pacing cycle lengths of 600-2000 ms. This is in range of improvement in CV calculated for the changes in I_{Na} observed in the DOCA mouse myocytes with NAD⁺ treatment (i.e. 1.08). Despite the consistency with the mouse model and the likely salutary nature of improving conduction, we cannot rule out that NAD⁺ had other effects that improved CV aside from increasing I_{Na}.

In the study of the GPD1L A280V mutant, NAD⁺ and mitoTEMPO were able to reverse the phenotype and reduce spontaneously induced arrhythmias in a mouse model of Brugada Syndrome [9]. In this work, we found that these compounds had analogous effects to raise I_{Na} in the nonischemic cardiomyopathy DOCA model. Treating either myocytes directly or the animal, NAD⁺ and mitoTEMPO were able to reduce mitochondrial ROS overproduction and rectify the decreased I_{Na}. This suggests that while there may be other sources of oxidative stress in this cardiomyopathy model, mitochondrial ROS are most important for the reduction in I_{Na}. Interestingly, mitoTEMPO has also been tested in DOCA mice that show hypertension and resulted in reduced blood pressure [39].

NAD⁺, in a redox couple with NADH, has emerged as a putative metabolic regulator of transcription, longevity and several age-associated diseases, including diabetes, cancer and neurodegenerative diseases.[40] In our previous studies and this work, we have shown that extracellular NAD⁺ increases cardiac Na_v1.5 currents and reduces antiarrhythmic risk in SCN5A^{+/-} hearts, a condition mimicking BrS.[9, 10] Nevertheless, NAD⁺ is impermeable to cell membrane. Extracellular NAD⁺ effects on intracellular signaling have been observed, and there are at least three candidates that may transmit the NAD⁺ signaling from the plasma to the cytosol. They are the β-AR, CD38, and the purinergic receptor [13-16]. We identified CD38 as the main agent to transduce extracellular NAD⁺ signaling. The ectoenzyme CD38 is a plasma membrane glycoprotein and has been reported to be a NAD⁺ and cyclic ADP-ribose (cADPR) transporter [16, 41, 42]. In addition, it catalyses intracellular cADPR synthesis from NAD⁺. In our recent unpublished work, we have also found that an antagonist of cADPR, 8-Br-cADPR, impaired the effects of NAD⁺ and forskolin on recovering I_{Na} in HEK cells stably expressing the human cardiac Na_v1.5. These results are consistent with CD38 mediating the NAD⁺ effect.

We examined the involvement of PKA and PKC in the reduction of I_{Na} and overproduction of

mitochondrial ROS in DOCA mouse myocytes with forskolin, chelerythrine, and δ V1-1. They enhanced I_{Na} and blunted the elevated mitochondrial ROS level of DOCA mouse myocytes. This indicates that, similar to the mechanism we have found in the mutant A280V GDP1L modulation of the cardiac $Na_v1.5$ [9, 10], PKC activation participates in the signaling pathway decreasing the I_{Na} in DOCA mice myocytes, and that PKA activation can be used to upregulate cardiomyocyte $Na_v1.5$ of DOCA mice by inhibiting mitochondrial ROS overproduction. In a study of the vertebrate brain type IIA Na^+ channel expressed in *Xenopus* oocytes on single channel level, the open time constant decreased from 0.26 ± 0.05 ms to 0.17 ± 0.03 ms with treatment of 5 nM phorbol 12-myristate 13-acetate (PMA, a PKC activator) at -50 mV [43]. Treatment of PMA also led to a reduced peak Na^+ current, reduced channel open probability, and prolonged time constants for channel activation. A reduction in I_{Na} secondary to changes in channel gating is consistent with our observations that $Na_v1.5$ mRNA and membrane protein were unchanged with cardiomyopathy or treatment. In data not shown, a specific inhibitor for calcium/calmodulin-dependent protein kinase II (CaMKII), autocamtide-2 related inhibitory peptide (AIP) at 500 nM, could not block the NADH effect on reducing I_{Na} . Therefore, it would seem unlikely that CaMKII plays a significant role in the observed reduction in I_{Na} during nonischemic cardiomyopathy.

Mitochondria comprise ~30-40% of the myocyte volume, generate >90% of the ATP [44, 45], and play a key role in many cellular functions including energy production, ion homeostasis, and cell signaling of cardiomyocytes. Mitochondria are one of the major sources of ROS in heart disease [46]. It is not surprising to find that mitochondrial dysfunction plays a critical role in nonischemic cardiomyopathy. Mitochondrial dysfunction can result in overproduction of ROS, acute energy failure, and cell death [47]. For example, a study of canine heart failure showed a decrease in the enzymatic activity of the complex I of the mitochondrial electron transport chain in heart failure, which caused the functional uncoupling of the respiratory chain and ROS overproduction [48]. In ischemia/reperfusion injury, the complex I serves as the source of ROS [49]. Mitochondrial injury occurring in ischemia is associated with increased NADH and ROS levels [11, 12].

It is unclear whether ROS participates directly in channel regulation or a second messenger pathway. The most vulnerable target of the posttranslational redox modifications to proteins is protein cysteine thiols, the oxidation of which may result in reversible molecular disulfide formation or other thiol modifications such as nitrosylation and glutathionylation [50-53]. In this study of the nonischemic cardiomyopathy model of 6-week DOCA mice, we observed a ~3-fold of mitochondrial ROS overproduction, which participated in the downregulation of cardiac $Na_v1.5$ function in an unknown mechanism. The specific mitochondrial ROS scavenger, mitoTEMPO curbed the mitochondrial ROS formation and reinstated I_{Na} to the level of sham mice. PKC inhibitors, chelerythrine and δ V1-1, were able to diminish the overproduction of mitochondrial ROS and restore the decreased I_{Na} of DOCA mouse myocytes, indicating that mitochondrial ROS generation is regulated by PKC in this cardiomyopathy heart model. NAD^+ and forskolin showed similar regulations on the mitochondrial ROS and I_{Na} levels of DOCA mouse myocytes as PKC inhibitors. On the other hand, both PKC and PKA-mediated phosphorylation has been shown to regulate the channel directly [54, 55]. It is possible that these kinases are both up and downstream of mitochondrial ROS production or that ROS-dependent modifications and phosphorylation interact at the channel to modulate current. Further experiments will be needed to differentiate these possibilities.

It is well recognized that increasing severity of myopathy parallels sudden death risk [56] and reduced I_{Na} increases arrhythmic risk [57]. These studies suggest that myopathy is linked directly to reduced I_{Na} and describe a mechanism whereby myopathy leads to metabolic derangements and increased mitochondrial ROS production causing the reduced I_{Na} . This work suggests a reduction in mitochondrial ROS in cardiomyopathy will reverse the reduced I_{Na} and possibly some of the arrhythmic risk by improving conduction velocity.

Disclosures

Dr. Dudley has filed provisional patents: 1) Modulation of sodium current by nicotinamide adenine dinucleotide and 2) Modulating mitochondrial reactive oxygen species to increase cardiac sodium channel current and mitigate sudden death, related to this work.

Acknowledgements

We thank Dr. Sergey Dikalov (Emory University, Atlanta, GA) for the gift of mitoTEMPO. This work was supported by NIH R01 HL085558, R01 HL072742, R01 HL106592, R01 HL104025, NIH R01 HL085369, T32 HL072742, and P01 HL058000 (SCD), and VA MERIT.

References

- [1] Bardy GH, Lee KL, Mark DB, Poole JE, Packer DL, Boineau R et al. Amiodarone or an implantable cardioverter-defibrillator for congestive heart failure. *N Engl J Med* 2005;352:225-37.
- [2] Kamphuis HCM, de Leeuw JRJ, Derksen R, Hauer RNW, Winnubst JAM. Implantable cardioverter defibrillator recipients: quality of life in recipients with and without ICD shock delivery. *Europace* 2003;5:381-9.
- [3] Thomas SA, Friedmann E, Kao CW, Inguito P, Metcalf M, Kelley FJ et al. Quality of life and psychological status of patients with implantable cardioverter defibrillators. *Am J Crit Care* 2006;15:389-98.
- [4] Valdivia CR, Chu WW, Pu J, Foell JD, Haworth RA, Wolff MR et al. Increased late sodium current in myocytes from a canine heart failure model and from failing human heart. *J Mol Cell Cardiol* 2005;38:475-83.
- [5] Ufret-Vincenty CA, Baro DJ, Lederer WJ, Rockman HA, Quinones LE, Santana LF. Role of sodium channel deglycosylation in the genesis of cardiac arrhythmias in heart failure. *J Biol Chem* 2001;276:28197-203.
- [6] Pu J, Boyden PA. Alterations of Na⁺ currents in myocytes from epicardial border zone of the infarcted heart. A possible ionic mechanism for reduced excitability and postrepolarization refractoriness. *Circ Res* 1997;81:110-9.
- [7] Baba S, Dun W, Boyden PA. Can PKA activators rescue Na⁺ channel function in epicardial border zone cells that survive in the infarcted canine heart? *Cardiovasc Res* 2004;64:260-7.
- [8] Shaw RM, Rudy Y. Ionic mechanisms of propagation in cardiac tissue: roles of the sodium and L-type calcium currents during reduced excitability and decreased gap junction coupling. *Circ Res* 1997;81:727-41.
- [9] Liu M, Sanyal S, Gao G, Gurung IS, Zhu X, Gaconnet G et al. Cardiac Na⁺ current regulation by pyridine nucleotides. *Circ Res* 2009;105:737-45.
- [10] Liu M, Liu H, Dudley SC, Jr. Reactive oxygen species originating from mitochondria regulate the cardiac sodium channel. *Circ Res* 2010;107:967-74.
- [11] Aon MA, Cortassa S, Marban E, O'Rourke B. Synchronized whole cell oscillations in mitochondrial metabolism triggered by a local release of reactive oxygen species in cardiac myocytes. *J Biol Chem* 2003;278:44735-44.
- [12] Di LF, Menabo R, Canton M, Barile M, Bernardi P. Opening of the mitochondrial permeability transition pore causes depletion of mitochondrial and cytosolic NAD⁺ and is a causative event in the death of myocytes in postischemic reperfusion of the heart. *J Biol Chem* 2001;276:2571-5.
- [13] Lu T, Lee H, Kabat J, Shibata EF. Modulation of rat cardiac sodium channel by the stimulatory G protein α -subunit. *J Physiol* 1999;518:371-84.
- [14] Bruzzone S, Moreschi I, Guida L, Usai C, Zocchi E, De-áflora A. Extracellular NAD⁺ regulates intracellular calcium levels and induces activation of human granulocytes. *Biochem J* 2006;393:697-704.
- [15] Romanello M, Padoan M, Franco L, Veronesi V, Moro L, D'Andrea P. Extracellular NAD⁺ induces calcium signaling and apoptosis in human osteoblastic cells. *Biochem Biophys Res Commun* 2001;285:1226-31.
- [16] Ying W, Garnier P, Swanson RA. NAD⁺ repletion prevents PARP-1-induced glycolytic blockade and cell death in cultured mouse astrocytes. *Biochem Biophys Res Commun* 2003;308:809-13.
- [17] Silberman GA, Fan T-H, Liu H, Jiao Z, Xiao HD, Lovelock JD et al. Uncoupled cardiac nitric oxide synthase mediates diastolic dysfunction. *Circulation* 2010;121:519-28.
- [18] O'Connor DT, Rodrigo M, Simpson P. Isolation and culture of adult mouse cardiac myocytes. *Methods Mol Biol* 2007;357:271-96.
- [19] Bogdanov KY, Vinogradova TM, Lakatta EG. Sinoatrial nodal cell ryanodine receptor and Na⁺-Ca²⁺ exchanger : molecular partners in pacemaker regulation. *Circ Res* 2001;88:1254-8.

- [20] London B, Michalec M, Mehdi H, Zhu X, Kerchner L, Sanyal S et al. Mutation in glycerol-3-phosphate dehydrogenase 1-like gene (GPD1-L) decreases cardiac Na⁺ current and causes inherited arrhythmias. *Circulation* 2007;116:2260-8.
- [21] Lou Q, Fedorov VV, Glukhov AV, Moazami N, Fast VG, Efimov IR. Transmural heterogeneity and remodeling of ventricular excitation-contraction coupling in human heart failure / clinical perspective. *Circulation* 2011;123:1881-90.
- [22] Fedorov VV, Glukhov AV, Ambrosi CM, Kostecki G, Chang R, Janks D et al. Effects of K_{ATP} channel openers diazoxide and pinacidil in coronary-perfused atria and ventricles from failing and non-failing human hearts. *J Mol Cell Cardiol* 2011;51:215-25.
- [23] Laughner JI, Sulkin MS, Wu Z, Deng CX, Efimov IR. Three potential mechanisms for failure of high intensity focused ultrasound ablation in cardiac tissue/clinical perspective. *Circ: Arrhythm Electrophysiol* 2012;5:409-16.
- [24] Bayly P, KenKnight B, Rogers J, Hillsley R, Ideker R, Smith W. Estimation of conduction velocity vector fields from epicardial mapping data. *IEEE Trans Biomed Eng* 1998;45:563-71.
- [25] Landmesser U, Dikalov S, Price SR, McCann L, Fukai T, Holland S et al. Oxidation of tetrahydrobiopterin leads to uncoupling of endothelial cell nitric oxide synthase in hypertension. *J Clin Invest* 2003;111:1201-9.
- [26] Kellenberger E, Kuhn I, Schuber F, Muller-Steffner H. Flavonoids as inhibitors of human CD38. *Bioorg Med Chem Lett* 2011;21:3939-42.
- [27] López-Sendón J, Swedberg K, McMurray J, Tamargo J, Maggioni A, Dargie H et al. Expert consensus document of b-adrenergic receptor blockers. *Eur Heart J* 2004;25:1341-62.
- [28] Wang DW, Mistry AM, Kahlig KM, Kearney JA, Xiang J, George AL. Propranolol blocks cardiac and neuronal voltage-gated sodium channels. *Front Pharmacol* 2010;1:144.
- [29] Moreschi I, Bruzzone S, Nicholas RA, Fruscione F, Sturla L, Benvenuto F et al. Extracellular NAD⁺ Is an Agonist of the Human P2Y₁₁ Purinergic Receptor in Human Granulocytes. *J Biol Chem* 2006;281:31419-29.
- [30] Umapathy NS, Zemskov EA, Gonzales J, Gorshkov BA, Sridhar S, Chakraborty T et al. Extracellular β-nicotinamide adenine dinucleotide (β-NAD) promotes the endothelial cell barrier integrity via PKA- and EPAC1/Rac1-dependent actin cytoskeleton rearrangement. *J Cell Physiol* 2010;223:215-23.
- [31] Glukhov AV, Fedorov VV, Kalish PW, Ravikumar VK, Lou Q, Janks D et al. Conduction remodeling in human end-stage nonischemic left ventricular cardiomyopathy/clinical perspective. *Circulation* 2012;125:1835-47.
- [32] Abriel H. Cardiac sodium channel Na_v1.5 and its associated proteins. *Arch Mal Coeur Vaiss* 2007;100:787-93.
- [33] Shibata EF, Brown TL, Washburn ZW, Bai J, Revak TJ, Butters CA. Autonomic regulation of voltage-gated cardiac ion channels. *J Cardiovasc Electrophysiol* 2006;17 Suppl 1:S34-S42.
- [34] Akai J, Makita N, Sakurada H, Shirai N, Ueda K, Kitabatake A et al. A novel SCN5A mutation associated with idiopathic ventricular fibrillation without typical ECG findings of Brugada syndrome. *FEBS Lett* 2000;479:29-34.
- [35] Brugada P, Brugada R, Brugada J. The Brugada syndrome. *Curr Cardiol Rep* 2000;2:507-14.
- [36] Makiyama T, Akao M, Tsuji K, Doi T, Ohno S, Takenaka K et al. High risk for bradyarrhythmic complications in patients with Brugada syndrome caused by SCN5A gene mutations. *J Am Coll Cardiol* 2005;46:2100-6.
- [37] Beswick RA, Zhang H, Marable D, Catravas JD, Hill WD, Webb RC. Long-term antioxidant administration attenuates mineralocorticoid hypertension and renal inflammatory response. *Hypertension* 2001;37:781-6.
- [38] Beswick RA, Dorrance AM, Leite R, Webb RC. NADH/NADPH oxidase and enhanced superoxide production in the mineralocorticoid hypertensive rat. *Hypertension* 2001;38:1107-11.
- [39] Dikalova AE, Bikineyeva AT, Budzyn K, Nazarewicz RR, McCann L, Lewis W et al. Therapeutic targeting of mitochondrial superoxide in hypertension. *Circ Res* 2010;107:106-16.

- [40] Lin SJ, Guarente L. Nicotinamide adenine dinucleotide, a metabolic regulator of transcription, longevity and disease. *Curr Opin Cell Biol* 2003;15:241-6.
- [41] Franco L, Guida L, Bruzzone S, Zocchi E, Usai C, Flora AD. The transmembrane glycoprotein CD38 is a catalytically active transporter responsible for generation and influx of the second messenger cyclic ADP-ribose across membranes. *FASEB J* 1998;12:1507-20.
- [42] Guida L, Bruzzone S, Sturla L, Franco L, Zocchi E, De Flora A. Equilibrative and concentrative nucleoside transporters mediate influx of extracellular cyclic ADP-ribose into 3T3 murine fibroblasts. *J Biol Chem* 2002;277:47097-105.
- [43] Schreibley W, Dascal N, Lotan I, Wallner M, Weigl L. Molecular mechanism of protein kinase C modulation of sodium channel α -subunits expressed in *Xenopus* oocytes. *FEBS Lett* 1991;291:341-4.
- [44] Murphy E, Steenbergen C. Preconditioning: the mitochondrial connection. *Annu Rev Physiol* 2007;69:51-67.
- [45] Barth E, Stämmler G, Speiser B, Schaper J. Ultrastructural quantitation of mitochondria and myofilaments in cardiac muscle from 10 different animal species including man. *J Mol Cell Cardiol* 1992;24:669-81.
- [46] Das DK, Maulik N. Mitochondrial function in cardiomyocytes: target for cardioprotection. *Curr Opin Anaesthesiol* 2005;18:77-82.
- [47] Duchen MR. Contributions of mitochondria to animal physiology: from homeostatic sensor to calcium signalling and cell death. *J Physiol* 1999;516:1-17.
- [48] Ide T, Tsutsui H, Kinugawa S, Utsumi H, Kang D, Hattori N et al. Mitochondrial electron transport complex I is a potential source of oxygen free radicals in the failing myocardium. *Circ Res* 1999;85:357-63.
- [49] Andrukhiv A, Costa ADT, West I, Garlid KD. Opening mitoK_{ATP} increases superoxide generation from complex I of the electron transport chain. *Am J Physiol Heart Circ Physiol* 2006;291:H2067-H2074.
- [50] Eaton P. Protein thiol oxidation in health and disease: techniques for measuring disulfides and related modifications in complex protein mixtures. *Free Radic Biol Med* 2006;40:1889-99.
- [51] Winterbourn CC. Reconciling the chemistry and biology of reactive oxygen species. *Nat Chem Biol* 2008;4:278-86.
- [52] Santos CXC, Anilkumar N, Zhang M, Brewer AC, Shah AM. Redox signaling in cardiac myocytes. *Free Radic Biol Med* 2011;50:777-93.
- [53] Lovelock JD, Monasky MM, Jeong EM, Lardin HA, Liu H, Patel BG et al. Ranolazine improves cardiac diastolic dysfunction through modulation of myofilament calcium sensitivity. *Circ Res* 2012;110:841-50.
- [54] Zhou J, Shin HG, Yi J, Shen W, Williams CP, Murray KT. Phosphorylation and putative ER retention signals are required for protein kinase A-mediated potentiation of cardiac sodium current. *Circ Res* 2002;91:540-6.
- [55] Tateyama M, Kurokawa J, Terrenoire C, Rivolta I, Kass RS. Stimulation of protein kinase C inhibits bursting in disease-linked mutant human cardiac sodium channels. *Circulation* 2003;107:3216-22.
- [56] Epstein AE, DiMarco JP, Ellenbogen KA, Estes III NAM, Freedman RA, Gettes LS et al. ACC/AHA/HRS 2008 guidelines for device-based therapy of cardiac rhythm abnormalities: a report of the American College of Cardiology/American Heart Association Task Force on practice guidelines (writing committee to revise the ACC/AHA/NASPE 2002 guideline update for implantation of cardiac pacemakers and antiarrhythmia devices) developed in collaboration with the American Association for Thoracic Surgery and Society of Thoracic Surgeons. *J Am Coll Cardiol* 2008;117:e350-e408.
- [57] Ruan Y, Liu N, Priori SG. Sodium channel mutations and arrhythmias. *Nat Rev Cardiol* 2009;6:337-48.

Table 1. Blood pressure and echocardiographic comparison between DOCA and sham mice

	Sham		DOCA		P value
	Value	N	Value	N	
Heart rate (bpm)	528 ± 17	4	533 ± 28	5	NS
SBP (mmHg)	99 ± 7	4	116 ± 3	5	< 0.05
DBP (mmHg)	74 ± 5	4	89 ± 3	5	< 0.05
LVESV (μL)	42.1 ± 3.6	8	64.6 ± 3.3	8	< 0.05
LVEDV (μL)	87.9 ± 6.1	8	104.7 ± 3.9	8	< 0.05
FS (%)	26.4 ± 1.0	8	17.9 ± 1.0	8	< 0.05
EF (%)	49.4 ± 3.7	8	37.1 ± 1.8	8	< 0.05

Note: SBP: systolic artery blood pressure; DBP: diastolic artery blood pressure; LVESV: left ventricular end-systolic volume; LVEDV: left ventricular end-diastolic volume; FS: fractional shortening; EF: ejection fraction. Values were compared between DOCA and sham mice at 6 weeks post surgery. N is the animal number used.

Table 2. The mean values of conduction velocity (cm/s) of human failing and normal heart before and after NAD⁺ treatment.

	Pacing Cycle Length (ms)			
	2000	1000	800	600
Control heart	49.2 ± 0.2	47.4 ± 0.7	51.7 ± 0.6	47.1 ± 4.5
Control heart + NAD ⁺	47.4 ± 0.7	47.2 ± 1.4	46.7 ± 1.9	47.5 ± 3.1
Failing heart	38.7 ± 2.1	35.8 ± 3.1	34.6 ± 2.8	33.8 ± 3.2
Failing heart + NAD ⁺	41.5 ± 2.2*	38.6 ± 3.0	37.0 ± 2.3*	35.5 ± 3.3*
Ratio of Failing/Control	0.79 ± 0.04	0.76 ± 0.07	0.67 ± 0.05	0.72 ± 0.1
Ratio of Failing + NAD ⁺ /Failing	1.07 ± 0.08	1.08 ± 0.13	1.07 ± 0.11	1.05 ± 0.14

Note: *P<0.05 vs failing heart group.

Figure captions

Fig 1 Increased NADH levels of the whole cell and cytosol were observed in DOCA mice, and injection of NAD⁺ to DOCA mice decreased the cytosolic NADH level that of sham mice. (A) Whole cell NADH and NAD⁺ levels, and the NADH/NAD⁺ ratio were obtained with the heart tissue of sham and DOCA mice. (B) Cytosolic NADH and NAD⁺ levels and the NADH/NAD⁺ ratio were measured from hearts of sham and DOCA mice with and without injected with NAD⁺. *P<0.01 vs. sham.

Fig. 2 Decreased I_{Na} was seen in DOCA cardiomyopathic mice. (A) Representative whole cell current traces of I_{Na} from sham and DOCA mouse ventricular cardiomyocytes held at -100 mV and measured from -100 to +60 mV with 10 mV steps. (B) Peak I_{Na} from sham and DOCA mice ventricular cardiomyocytes measured at -20 mV. *P<0.01 vs. sham.

Fig. 3 Na_v1.5 membrane expression measured with biotinylation was unchanged between sham and DOCA mice. The upper panel shows representative Western blots results for biotinylated Na⁺ channels. In these Western blots, β-actin was used as a loading control. The lower panel presents the averaged data showing no significant change of Na_v1.5 protein membrane expression in DOCA mice cardiomyocytes compared to the sham group.

Fig. 4 Reduced I_{Na} in cardiomyopathy was corrected by NAD⁺ or mitoTEMPO without significant changes in channel gating. (A, B, C) NAD⁺, mitoTEMPO, chelerythrine, or forskolin (500, 10, 50, or 5 μM, respectively) applied intracellularly to isolated cardiomyocytes restored the decreased I_{Na} in cardiomyopathic DOCA myocytes. (D, E, F) DOCA mice injected with NAD⁺ or mitoTEMPO (100 or 0.7 mg/kg, respectively) showed recovered I_{Na}. The minor shifts of V_{1/2} values of steady state gating were not enough to affect the evaluation of the peak currents. * P<0.01 vs. sham group.

Fig. 5 Mitochondrial ROS levels were increased in DOCA myopathic mice and reduced by NAD⁺, mitoTEMPO, δV1-1 and forskolin. (A) Mitochondrial ROS overproduction was observed with DOCA mice myocytes by MitoSOXTM Red (2.9±0.3-fold of sham, P<0.01) in confocal microscopy. DOCA cardiomyocyte treatment with NAD⁺, mitoTEMPO, δV1-1, or forskolin (500, 10, 2, or 5 μM, respectively) extracellularly decreased ROS levels in DOCA mouse myocytes to the level of sham group (1.4±0.1, 1.1±0.1, 0.9±0.1, or 0.8±0.1-fold of sham, respectively, P>0.05). Three to five animals were tested in each group, and total 29-43 cells were used for average. (B) DOCA mice injected with NAD⁺ (100 mg/kg) or mitoTEMPO (0.7 mg/kg) showed decreased mitochondrial ROS (1.1±0.1- or 1.1±0.2-fold of sham, respectively, P>0.05). Three to four animals and ~10000 myocytes from each animal were tested in each group in flow cytometry. (C) Representative confocal microscopy images from panel A were obtained with treatment of myocytes monitored with MitoTrackerTM Green and MitoSOXTM Red. The white scale bar is 20 μm. The extremely red cells are dying myocytes that had very high levels of ROS.

Fig 6. Optical mapping of failing human myocardium. (A) Representative left ventricular wedge preparation with key features highlighted. White dotted line – outlines field of view for activation and conduction velocity maps (C and D); blue and green circles – location of optical action potentials (B); pink asterisk – location of pacing stimulus; teal box – boundary of conduction velocity calculation. (B) Representative optical action potentials. (C) Activation map showing spread of electrical activity across the transmural wedge in 35ms. (D) *Left* panel: Conduction velocity vectors (red) on top of gray scale activation map; *center* panel: magnification of teal box where conduction velocity calculations were taken; *right* panel: summary of the conduction velocity of failing hearts before (control) and after treatment (500 μM NAD⁺) conditions while pacing tissue at several cycle lengths (2000, 1000, 800, 600 ms).

Fig. 1

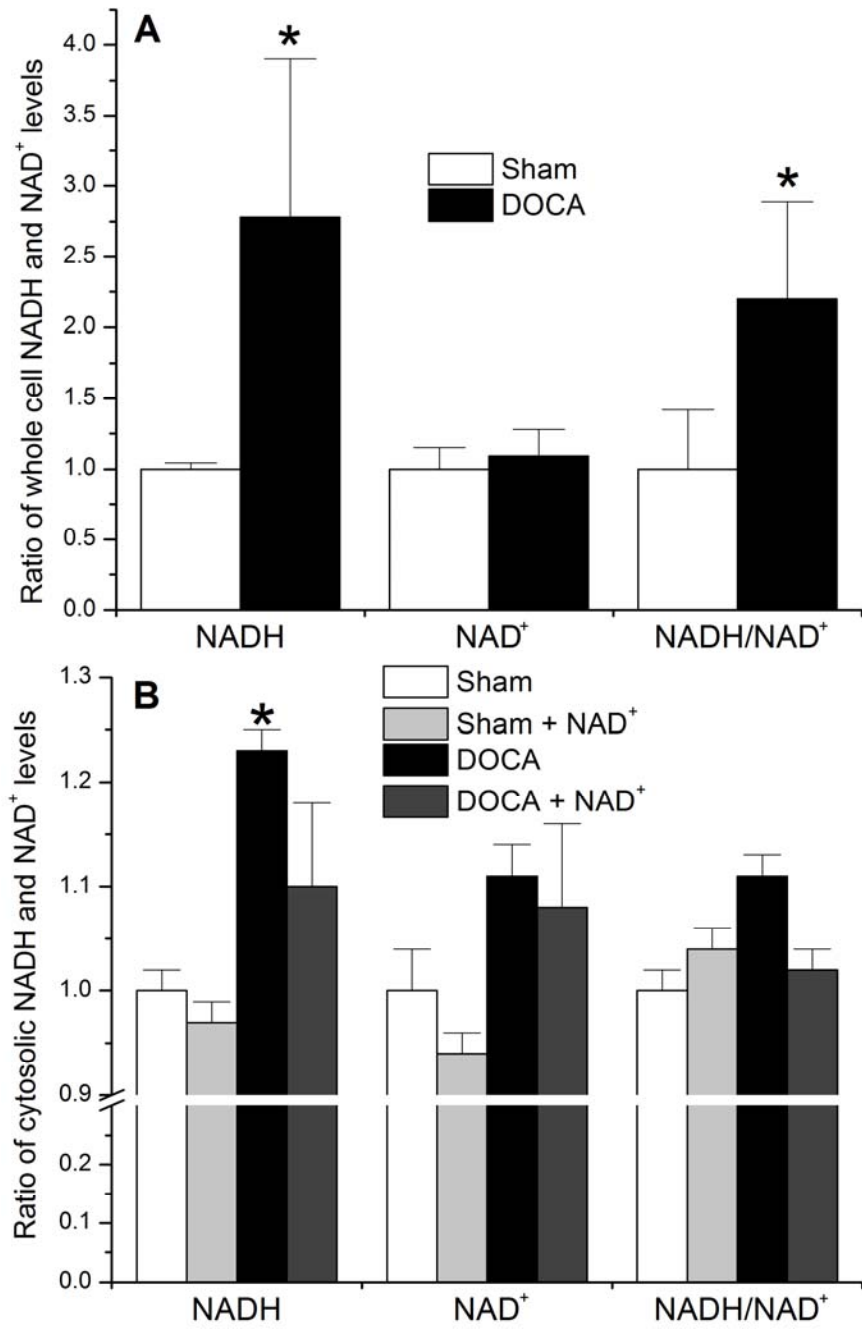


Fig. 2

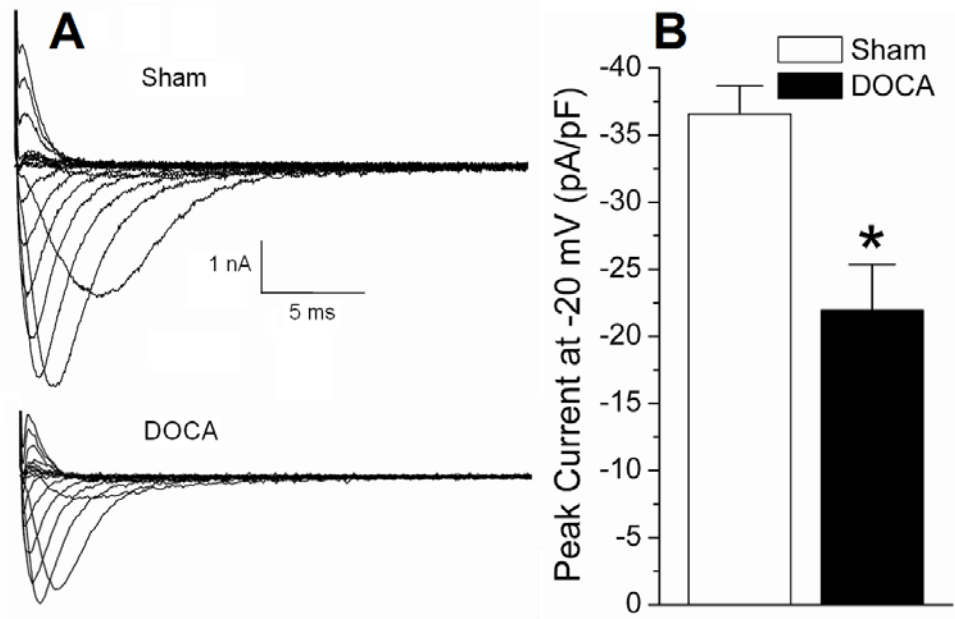


Fig. 3

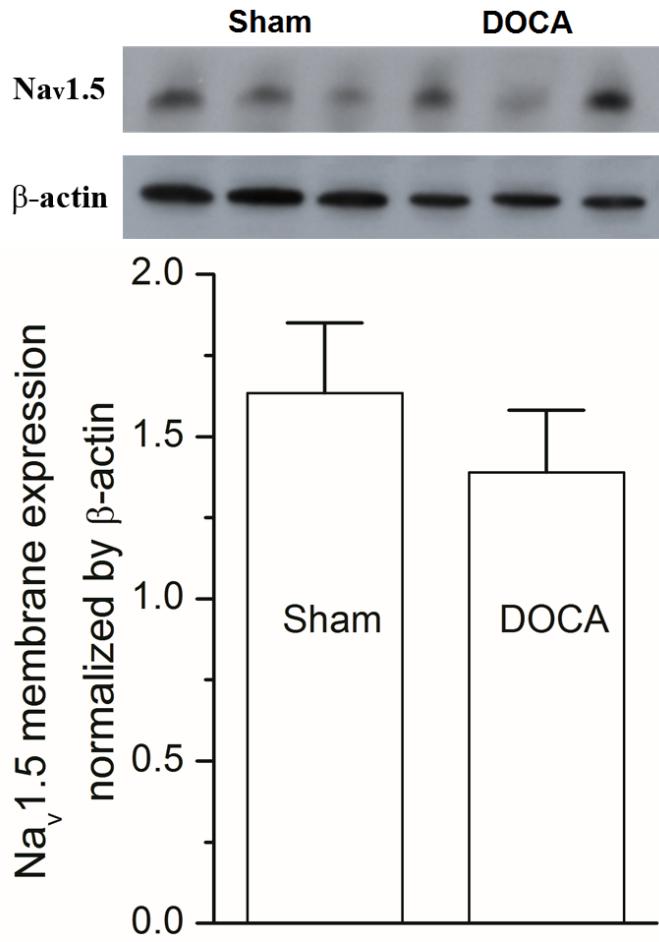


Fig. 4

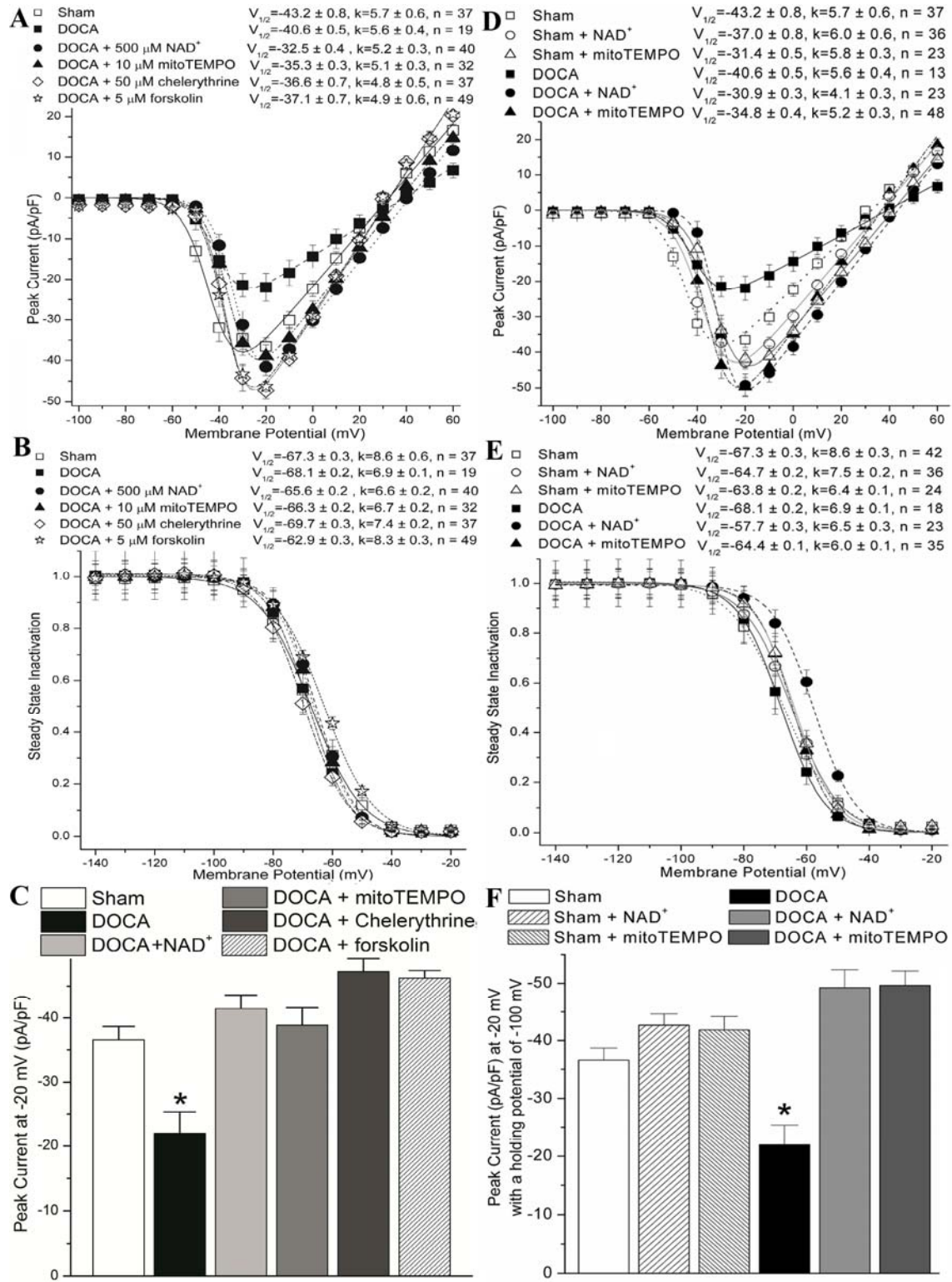


Fig. 5

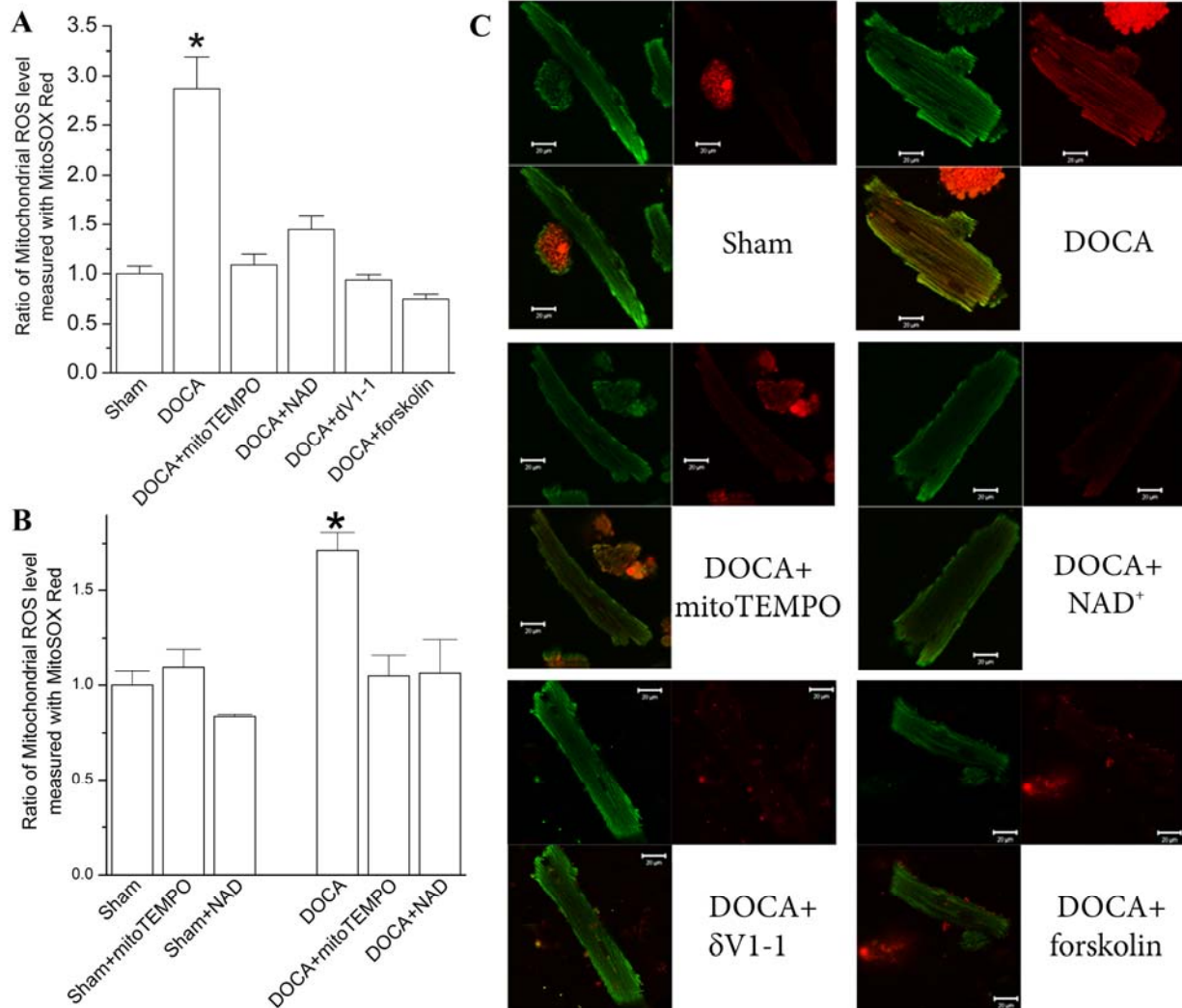


Fig. 6

